Nuclear Engineering and Technology 55 (2023) 364–372

Contents lists available at ScienceDirect

Nuclear Engineering and Technology

journal homepage: www.elsevier.com/locate/net

Original Article

Study on heat transfer characteristics and structural parameter effects of heat pipe with fins based on MOOSE platform

Xiaoquan Chen [a], Peng Du [b], Rui Tian [a], Zhuoyao Li [a], Hongkun Lian [c], Kun Zhuang [a, d], Sipeng Wang [a, d, *]

[a] Department of Nuclear Science and Technology, Nanjing University of Aeronautics and Astronautics, Nanjing, 211106, China
[b] Science and Technology on Reactor System Design Technology Laboratory, Nuclear Power Institute of China, Chengdu, 610213, China
[c] Changzhou Therma Tech Co. LTD, China
[d] Key Laboratory of Nuclear Technology Application and Radiation Protection in Astronautics (Nanjing University of Aeronautics and Astronautics), Ministry of Industry and Information Technology, China

ARTICLE INFO

Article history:
Received 20 June 2022
Received in revised form
23 August 2022
Accepted 21 September 2022
Available online 27 September 2022

Keywords:
Space reactor
Radiator
MOOSE
Heat dissipation power
Power-mass ratio

ABSTRACT

The space reactor is the primary energy supply for future space vehicles and space stations. The radiator is one of the essential parts of a space reactor. Therefore, the research on radiators can improve the heat dissipation power, reduce the quality of radiators, and make the space reactor smaller. Based on MOOSE multi-physics numerical calculation platform, a simulation program for the combination of heat pipe and fin at the end of heat pipe radiator is developed. It is verified that the calculation result of this program is accurate and the calculation speed is fast. Analyze the heat transfer characteristics of the combination with heat pipe and fin, and obtain its internal temperature field. Based on the calculation results, the influence of structural parameters on the heat dissipation power is analyzed. The results show that when the fin width is 0.25 m, fin thickness is 0.002 m, condensing section length is 0.5425 m and heat pipe radius is 0.014 m, the power-mass ratio is the highest. When the temperature is 700K–900K, the heat dissipation power increases 41.12% for every 100K increase in the operating temperature. Smaller fin width and thinner fin thickness can improve the power-mass ratio and reduce the radiator quality.

1. Introduction

Chemical energy, solar energy, and nuclear energy are the energy supply for aerospace engineering. Nuclear energy mainly comes from isotope batteries and space reactors. Compared with other energy sources, a space reactor has the advantages of long life, high energy density, and small volume, which is a crucial energy guarantee for human beings to enter the space era. As the heat dissipation system of a space reactor, the weight of radiator can account for about 40% of the space reactor, which seriously occupies the carrying weight. Therefore, optimizing radiator has become an essential direction of space reactor development.

The design schemes of radiator mainly include loop type, heat pipe type, and droplet type [1–4]. The Loop radiator has the advantages of lightweight and high heat dissipation power, but there is a single point of failure. Any coolant pipe rupture will lead to the collapse of whole cooling circuit. The droplet radiator has the advantages of small space occupation and easy stretching. However, it is still in the development stage, and the technology is immature. The heat pipe radiator [5–8] has the advantages of the initiative, high safety factor, and mature technology which is currently the most widely used radiation cooling scheme.

As shown in Fig. 1. The heat pipe radiator mainly uses the heat pipe to transfer heat to the radiating fin and dissipates heat into space through thermal radiation. Through experiments, Robert Richter [9] studied the influence of working pressure and temperature on heat transfer of mercury heat pipes. Yaleeastman [10] studied the effect of air impurities inside the heat pipe on the thermal conductivity of the heat pipe. Chul Hwan Yang [11] studied the relationship between working temperature and heat dissipation efficiency. Based on the thermal resistance model, Xiu Zhang [12] optimized the heat pipe space radiator's fin heat dissipation efficiency and system quality characteristics based on the thermal resistance model. Haochun Zhang [13]studied the effects of fin

* Corresponding author. Department of Nuclear Science and Technology, Nanjing University of Aeronautics and Astronautics, Nanjing, 211106, China.
E-mail address: wangsipeng@nuaa.edu.cn (S. Wang).

https://doi.org/10.1016/j.net.2022.09.022

Nomenclature

A	area, m^2
C	specific heat capacity, J/(kg·K)
d	diameter of the heat pipe, m
E	fin radiation intensity, W/m^2
h_{fg}	latent heat of vaporization, J/kg
k	heat transfer coefficient, W/(m2·K)
L	heat pipe length, m
m	quality, kg
p	pressure, Pa
P	total heat dissipation power, W
Q	heat transfer limit, W
r	heat pipe radius, m
R	thermal resistance, $K·m^2/W$
R_g	gas constant, J/(kg·K)
S	source item
t	time, s
T	temperature, K

Greek

ρ	density, kg/m^3
ϕ	heat flux, W
ψ	trial function
ε	emissivity
σ	Stefan-Boltzmann constant surface tension, $N·m^{-1}$
η	power-mass ratio
μ	dynamic viscosity, Pa·s
π	PI
λ	thermal conductivity, W/(m·K)
θ	poriness

Subscripts

b	blackbody
b	bubble
c	capillary
cma	critical molecular area
D	radiation surfaces
e	equivalent
ev	evaporator
eff	effective
f	working fluid
i	inner of shell
p	pressure
s	wick
v	vapor
w	radiator body
∞	space
Ω	total integral region

length and thickness, coolant mass flow rate and radiator inlet temperature on radiator quality under given working conditions by using the exhaustive method and genetic algorithm. It can be seen that the current research on heat pipe radiators has a certain research foundation. However, the current research is mainly carried out by thermal resistance network method or other methods, these methods can't get the fine distribution of heat pipe and fin temperature, and accurate research on heat pipe fin temperature is still lacking.

Based on MOOSE (Multiphysics Object-Oriented Simulation Environment), this paper develops a program for heat transfer numerical calculation of the combination of heat pipe and fin and verifies its correctness. Based on the program, the heat transfer calculation of the combination of heat pipe and fin with different fin thickness, width, length and heat pipe radius is carried out. The influence of various parameters on heat dissipation power is analyzed, which provides a reference for optimizing the radiator structure.

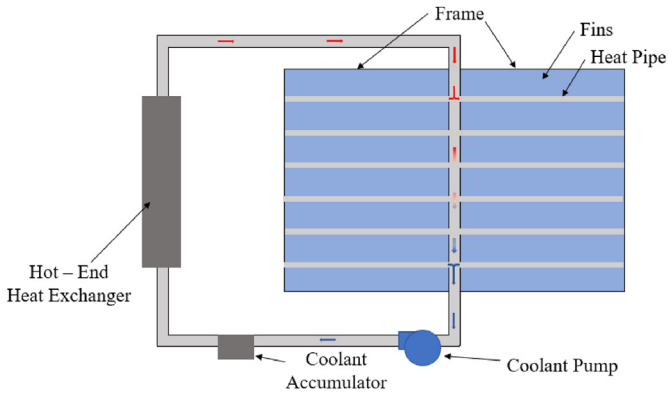

Fig. 1. Schematic diagram of the heat pipe radiator.

2. Model and methods

2.1. Introduction to MOOSE platform

MOOSE platform is an open-source general-purpose computing platform developed by the Idaho National Laboratory for multi-physics numerical computing problems. Based on the finite element method and PJFNK algorithm, it can efficiently and modularly solve partial differential equations. MOOSE platform has the characteristics of object-oriented, which can achieve cross-dimensional calculation. A set of codes can be used for different dimensions. MOOSE platform adopts an adaptive mesh for the model, and automatically enrich the mesh where refinement is needed. Based on the MOOSE platform, fuel performance analysis code, reactor physics calculation code, and system analysis code have been developed.

The MOOSE calculation program has three levels, as shown in Fig. 2. The bottom is the libmesh module and the solver module. The MOOSE platform inherits the open-source library of libmesh for mesh reading, finite element discretization, residual matrix formation, and result output. The residual matrix is solved by PJFNK or NEWTON method. The middle layer is the different modules of MOOSE, which supports various conditions in the top layer such as the physical problem boundary and material calculated. The top layer is the developer module, developed based on the middle definition module.

This program is based on the existing modules of heat conduction, thermal convection, material, and kernel on the MOOSE platform. It develops modules such as thermal radiation and power calculation to simulate the heat transfer of combination of heat pipe and fin.

2.2. Mathematical model

The heat conduction equation in heat pipe fins can be described by formula (1)

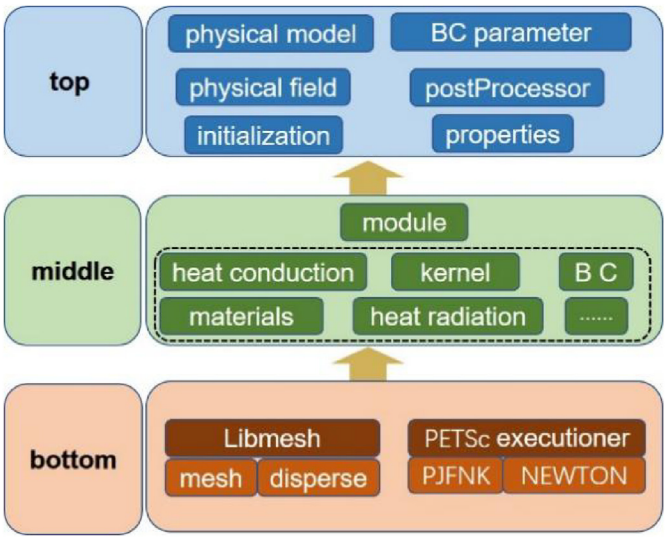

Fig. 2. Moose hierarchy diagram.

$$\rho C_p \frac{\partial T}{\partial t} + \nabla(-k\nabla t) - S = 0 \tag{1}$$

In Eq. (1), ρ is density, C_p is constant pressure specific heat capacity, T is temperature, t is time, k is the thermal conductivity, S is the source item.

MOOSE uses Galerkin's method to solve the governing equations of physical problems, which involves expressing the strong form of a governing equation in a weak form. The divergence theorem is applied to generate the boundary integral and the inner product notation is used to express the final weak form. The weak form of the heat conduction equation is shown by formula (2)

$$\left(\rho C_p \frac{\partial T}{\partial t}, \psi\right) + (k\nabla T, \nabla\psi) - (S, \psi) - \langle k\nabla T, \psi\rangle = 0 \tag{2}$$

In Eq. (2), ψ is a trial function. The first three terms represent the kernel used to inherit the MOOSE module in the weak form of the equation, and $\langle k\nabla T, \psi\rangle$ represents the boundary conditions.

The heat radiation equation in fins can be described as follows

$$\rho C_p \frac{\partial T}{\partial t} - \nabla^2 T - E = 0 \; \rho C_p \frac{\partial T}{\partial t} - \nabla^2 T - E = 0 \tag{3}$$

$$E = \varepsilon E_b = \varepsilon\sigma\left(T_w^4 - T_\infty^4\right) \tag{4}$$

In Eq. (3) and Eq. (4), E is the fin radiation intensity, $E_b$is the blackbody radiation intensity, ε is the emissivity, σ is the Stefan-Boltzmann constant, T_w is the object temperature, $T_\infty$is the external temperature.

The underlying solver uses the PETSc package built into MOOSE and the solution type is NEWTON. This method has been proved to be stable and fast. The spatial discretization scheme used on the MOOSE platform is as follows (5)

$$\int_\Omega f(x)dx = \sum_{cma} \int_{\Omega_{cma}} f(x)dx \tag{5}$$

In Eq. (5), Ω is the total integral region, Ω_{cma} is the sub-integral region, c is the label of the critical molecular area, and x is the essential point.

When analyzing the combination of heat pipe and fin, the radiator performance is determined by comparing its radiation heat dissipation power and power-mass ratio. The emphasis is obtained by the surface area of radiation heat flux (W/m^2) on all radiation heat dissipation surfaces, as shown in the formula

$$P = \iint_D E(T_w)dT_w \tag{6}$$

In Eq. 6, D for all radiation surfaces, $E(T_w)$ for different surface radiation heat flux. The power-mass ratio is defined as the combined mass of radiant heat dissipation power ratio (W/kg), as follows

$$\eta = \frac{P}{m} \tag{7}$$

2.3. Physical model

The working fluid of heat pipe absorbs heat to evaporate in evaporation section and releases heat to liquefy in condensation section. There are delicate components such as wick, wall, and working fluid. The simulation of heat pipe needs large amount of calculating, so it is necessary to simplify the heat pipe reasonably. This paper uses the solid heat conduction model to simulate the heat pipe. The steam chamber and the wick are equivalent to solid materials. The equivalent thermal conductivity of the steam chamber is obtained by calculating the thermal flow resistance of the steam chamber of the heat pipe. Compared with the commonly used thermal resistance network method, the solid heat conduction method can get more refined temperature distribution, rather than the temperature of only a few nodes, and the calculation speed is faster. The thermal resistance is shown as follows [14].

$$R = \frac{128 L_{eff}\mu T_v^2 R_g}{\pi\rho_v d_v^4 p_v h_{fg}^2} \tag{8}$$

In Eq. (8), L_{eff} is the effective length of the heat pipe, μ is the dynamic viscosity, d is the diameter of the heat pipe, h_{fg} is the latent heat of vaporization, R_g is the gas constant, p is the pressure.

It is assumed that the working medium in the heat pipe is completely melted under the steady state condition, and the heat pipe can be completely started. For the wick region, the flow of liquid in the wick is ignored, and the heat transfer process in this region is simplified to a pure heat conduction model assuming the heat transfer coefficient. The equivalent thermal conductivity of the wick is shown in the formula below [15].

$$\lambda_e = \frac{\lambda_f\left(\left(\left(\lambda_f + \lambda_s\right) - (1-\theta)\left(\lambda_f - \lambda_s\right)\right)\right)}{\left(\lambda_f + \lambda_s\right) + (1-\theta)\left(\lambda_f - \lambda_s\right)} \tag{9}$$

In Eq. (9), $\lambda_f$is the thermal conductivity of the working fluid, $\lambda_s$is the thermal conductivity of the wick, and θ is the porosity.

The equivalent density and heat capacity are shown as follows [16]

$$c_e\rho_e = \theta \cdot c_f\rho_f + (1-\theta)c_s\rho_s \tag{10}$$

In Eq. (10), c_e is equivalent heat capacity, ρ_e and is equivalent density.

The internal modeling of the heat pipe is complex, and the built-in modeling software of the MOOSE platform is not enough to support the modeling of complex geometry. Therefore, this paper uses Coreform Cubit software to establish the physical model. Cubit

is an advanced mesh generation software developed by Sandia National Laboratory for complex simulation problems, which can provide professional pre-simulation solutions. Because the equivalent heat conduction model is adopted, the wick and working medium of the heat pipe are equivalent to a solid material, so the porosity and shape of the wick are not considered in the modeling process, and the wick area is decomposed into several layers of mesh for calculation.

The model of combination with heat pipe and fin is shown in Fig. 3. The model is the end unit of the space heat pipe radiator. The heat pipe transmits the heat of the evaporation section to the condensation section, and the heat is transferred to the outside in the form of thermal radiation through the fins connected to the condensation section of the heat pipe, which has a good heat dissipation capacity. The specific parameters [17] are shown in Table .1.

2.4. Heat pipe heat transfer limit

Considering the capillary structure in the wick part of the heat pipe, the working medium is refluxed by capillary force. The capillary force of the capillary structure has a maximum value, so the heat transfer capacity of the heat pipe is also limited by the capillary structure. The calculation of its capillary limit is shown in Equation (11) [18]:

$$Q = \frac{2\sigma/r_c + \rho g L \sin\alpha}{L_{eff}\left(F_f + F_v\right)} \tag{11}$$

In Eq. (11), Q is capillary limit, σ is surface tension, $r_c$is capillary radius, $L$is the length of the heat pipe, $\alpha$is inclination angle of heat pipe, $F_f$is coefficient of friction of liquid, F_v is coefficient of friction of vapor.

Because the steam in the heat pipe flows very fast, the liquid will be carried by the gas into the steam chamber, thus limiting the heat transfer capacity. According to the equivalent hydraulic radius of the wick, the carrying limit is shown in Equation (12).

$$Q = A_v h_{fg}\sqrt{\rho_v \sigma / 2r_e} \tag{12}$$

In Eq. (12), Q is entrainment limit, A_v is wick cross-sectional area, σ is surface tension, $r_e$is equivalent hydraulic radius.

When the temperature of the evaporation section of the heat pipe is too high, the working medium in the suction core will boil and produce a large number of bubbles, which will hinder the flow and circulation of the liquid, and the boiling limit will appear. The boiling limit is shown in Equation (13).

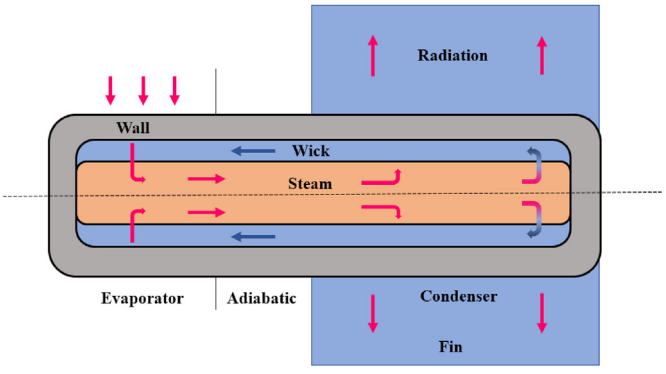

Fig. 3. Physical model.

Table 1
Design parameters of combination.

Parameter (m)	value
Heat pipe radius	0.016
Length of evaporator	0.105
Length of adiabatic	0.0525
Length of condenser	0.5425
Thickness of wick	0.001
Width of fins	0.25
Fin thickness	0.004

$$Q = \frac{2\pi L_{ev}\lambda_e T_v}{h_{fg}\rho_v \ln(r_i/r_v)}\left(\frac{2\sigma}{r_b} - \Delta p\right) \tag{13}$$

In Eq. (13), Q is boiling limit, σ is surface tension, $L_{ev}$is length of evaporation section, $r_i$is inner radius of shell, $r_v$is steam zone radius, $r_b$is critical bubble radius, Δp is capillary pressure drop.

Because the limit of sound speed mainly takes effect in low temperature heat pipes, and the heat pipes in this paper have high temperature, the limit of sound speed is not considered.

3. Analysis of calculation results

3.1. Program verification of solid heat conduction method

The solid heat conduction method is used to simplify the heat transfer of heat pipe. In order to verify the calculation accuracy of this method and the calculation accuracy of the program developed based on MOOSE, the heat transfer experimental data of heat pipe are selected to prove it. The parameters of the heat pipe model are consistent with those set by Chai et al. [19], and the boundary is set as follows

$$k\frac{\partial T_w}{\partial r}\bigg|_{r=r_0} = \frac{\phi}{A_{ev}}(evaporator) \tag{14}$$

$$k\frac{\partial T_w}{\partial r}\bigg|_{r=r_0} = 0(adiabatic) \tag{15}$$

$$-k_w\frac{\partial T_w}{\partial r}\bigg|_{r=r_0} = \begin{cases} h(T_w - T_\infty) \\ \sigma\varepsilon\left(T_w^4 - T_\infty^4\right) \end{cases} -k\frac{\partial T_w}{\partial r}\bigg|_{r=r_0} = \sigma\varepsilon\left(T_w^4 - T_\infty^4\right) \times (condenser) \tag{16}$$

The wall temperature and steam temperature are selected as the comparison object. The internal pressure of the heat pipe is 0.09 MPa. The experimental data is compared with the numerical calculation data. The results are shown in Fig. 4. The temperature curve of the developed program using the solid thermal conductivity method is consistent with the experimental results. The average temperature of the wall and steam is calculated by selecting the temperature measurement point, and the calculation results are shown in Table .2. The average temperature error between each section of the wall and potassium steam is less than 3 K, and the temperature error of the steam chamber is only 0.3 K. The results show that the calculated results are in good agreement with the experimental results. The feasibility of solid heat conduction method and the veracity of the program are verified.

3.2. Mesh independence analysis

In the numerical calculation of the combination, it is necessary to divide the mesh first. The mesh density will affect the calculation

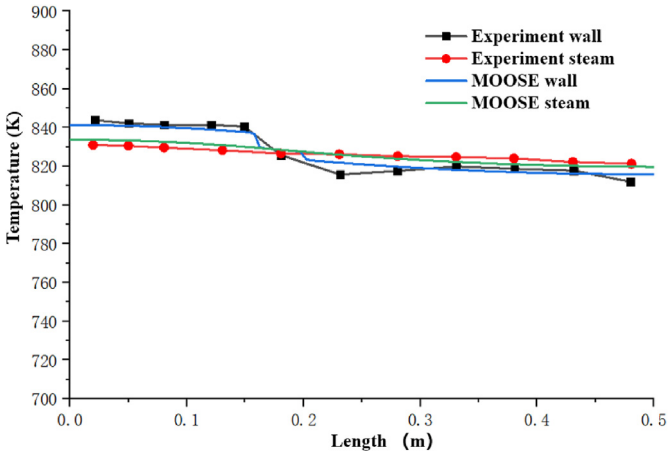

Fig. 4. Verification of heat pipe program.

speed and the accuracy of the results. Based on Coreform Cubit modeling software, the combined model is divided into eight meshes ranging from 5725 to 465,808. The temperature distributions of eight different meshing modes were compared and analyzed. The total heat dissipation power and the temperature curve at the top of the fin are shown in Fig. 5. The temperature and power errors of the three schemes with mesh smaller than 35,629 are large, while the temperature curves of the other mesh are basically the same, and the power tends to be the same. The results show that when the number of mesh is greater than 80,933, the temperature change is no longer obvious and the radiative heat dissipation power tends to be the same. Considering the calculation speed and accuracy, 261,140 mesh partition scheme is adopted in the subsequent mesh. Since the physical model will change, there will be some difference in the number of mesh in the future, but it does not affect the calculation.

3.3. Width of fins

Table 1 condition is set as the reference condition, and the influence of parameters is analyzed. The temperature distribution under the reference condition is shown in Fig. 6. The heat pipe steam temperature is 775.31 K, and the fin end temperature is 675.06 K. The radiation heat dissipation power is 3636.95 W, and the power-mass ratio is 2586.41 (W/kg). The heat transfer limit of the heat pipe under this condition is calculated. Compared with the capillary limit, the carrying limit and the boiling limit, the minimum value is 20246 W of the boiling limit, and the heat transfer power of the heat pipe is 3636.95 W, so the heat pipe could meet the heat transfer requirements.

The influence of fin width on heat dissipation efficiency at different temperatures is analyzed. The radiation power, power-mass ratio, and temperature distribution are shown in Fig. 7. As the fin widens, the heat dissipation area increases, the heat dissipation power increases, and the mass of the combination increases linearly. However, the temperature at the end of the fin is low, and the rising speed of the radiation heat dissipation power decreases continuously. Therefore, the power-mass ratio increases at the beginning, and then decreases. When the evaporation temperature is 700 K, the width of the maximum power-mass ratio is 0.25 m. When temperature of evaporation rises to 800 K, the power increases by 37.66%, and the fin width of the highest power-mass ratio remains unchanged. When temperature of evaporation rises to 900 K, the power increases by 44.64% compared with that at 800 K, and the power-mass ratio is the highest when the fin width is 0.2 m. As shown in Fig. 7, when the temperature of the evaporation section increases, the heat dissipation power also increases. The change of the fin temperature under high temperature condition is more obvious than that under low temperature condition. Therefore, the highest power-mass ratio can be achieved when the fin width is 0.2 m.

Table 2
Average temperature of heat pipe.

	Evaporator wall	Adiabatic wall	Condenser wall	steam
Experimental average temperature (K)	841.85	825.7	816.98	826.35
Numerical calculation temperature (K)	839.87	828.28	818.32	826.05
Error (K)	1.98	2.58	1.34	0.3
Relative error	0.24%	0.31%	0.16%	0.03%

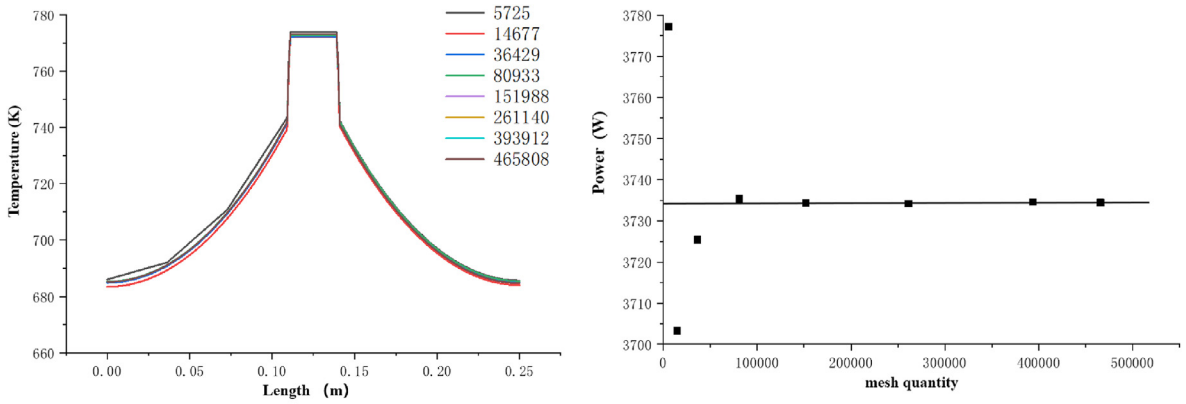

(a) Temperature curve (b) Radiant thermal power

Fig. 5. Mesh independence verification.

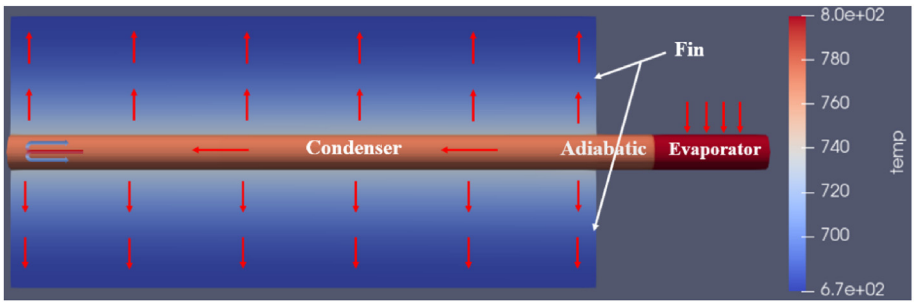

Fig. 6. Temperature distribution.

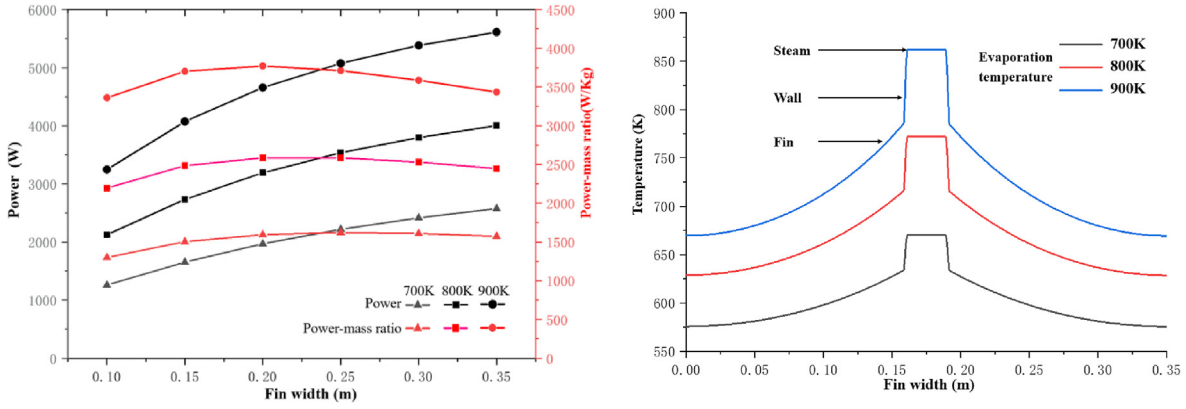

(a) Power, power-mass ratio curves (b) Fin temperature distribution

Fig. 7. Comparison of different widths.

3.4. Fin thickness

The influence of fin thickness at different temperatures on the heat dissipation efficiency is compared and analyzed. The radiation heat dissipation power and power-mass ratio are shown in Fig. 8. As the primary heat dissipation unit, the thermal resistance of fins decreases with the increase of fins thickness, the average temperature of the fin increases, and the heat dissipation power increases. The mass of the combination increases linearly, but the increased rate of the heat dissipation power will continue to slow down, so there is a maximum power-mass ratio. When temperature of evaporation is 700 K, the overall temperature of the fin is low. With the increase of thickness, the heat dissipation power increases slowly, and the power-mass ratio decreases gradually. When temperature at evaporation section is 800K, the heat dissipation power of the fin increases by 36.73%, and the power-mass ratio rises first and then decreases, reaching 2910.81(W/kg) when the thickness is 0.002 m. Temperature at evaporation section is 900 k, the heat dissipation power of the fin increases by 42.95%, and the thickness of the fin with the highest power-mass ratio remains unchanged. By comparing the power variation curves at different temperatures, it can be seen that the fin thickness has significant influence on the heat dissipation power of the fin at the higher temperature, and the high-temperature fin needs the fin with minor thermal resistance to maintain its high heat dissipation power.

The heat pipe does not change when the fin width is changed and the fin thickness is changed. The heat transfer limit of the heat pipe at different temperatures was calculated, as shown in Fig. 9. The boiling limit is the minimum. The maximum heat transfer power under the conditions of varying width and thickness is lower than the boiling limit of heat pipe. Therefore, all heat pipes can complete heat transfer.

3.5. Condensation length

The influence of condensation section length on the heat dissipation efficiency at different temperatures is compared and analyzed. The radiation heat dissipation power and power-mass ratio are shown in Fig. 10. The condensation section of the heat pipe is connected with the fin. With the increase of the condensation section, the length of the fin and the radiation dissipation area increases. Therefore, the heat dissipation power is greatly affected by the length of the condensation section. With the increase in the length of the condensation section, the mass of the combination increases linearly. Meanwhile, the temperature at the end of the condensation section decreases continuously. The rising speed of the heat dissipation power will slow down, so the power-mass ratio increases at the beginning, and then decreases. When temperature of evaporation is 700 K, the length of the maximum power-mass ratio is 0.5425 m. When temperature of evaporation rises to 800 K, the power increases by 37.07%. When temperature of evaporation rises to 900 K, the power increases by 43.94% compared with that at 800 K, and the length of the condensation section at the highest power-mass ratio remains unchanged.

By calculating the heat transfer limit of the heat pipe, it is found that the entrainment limit and boiling limit do not change, and the capillary limit decreases with the increase of the length of the heat pipe, but it is still larger than the boiling limit. Therefore, the maximum heat transfer power of the heat pipe under this condition is less than the heat transfer limit.

3.6. Radius of heat pipe

The internal structure of the heat pipe is complex, so it is necessary to simplify the heat pipe model reasonably. Without

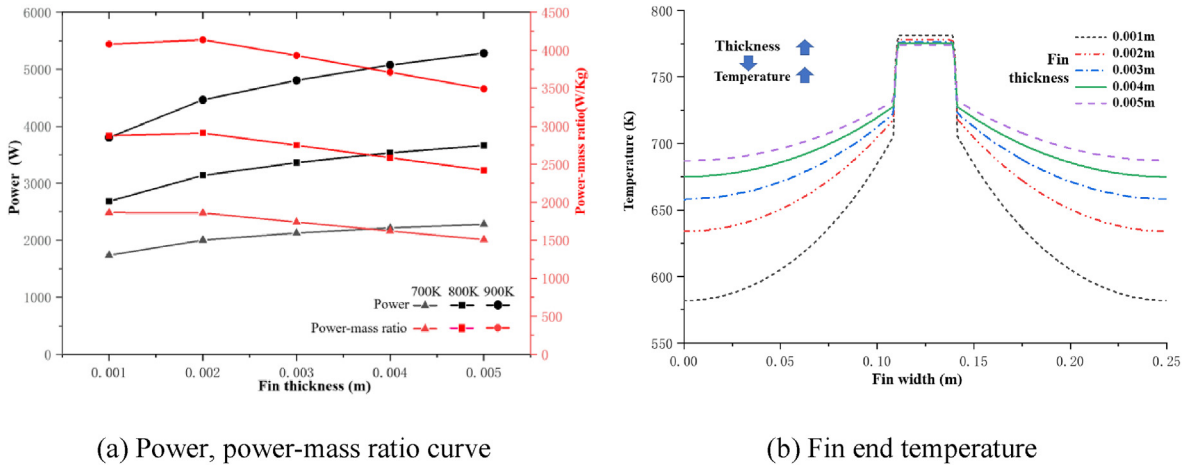

Fig. 8. Comparison of different thickness.

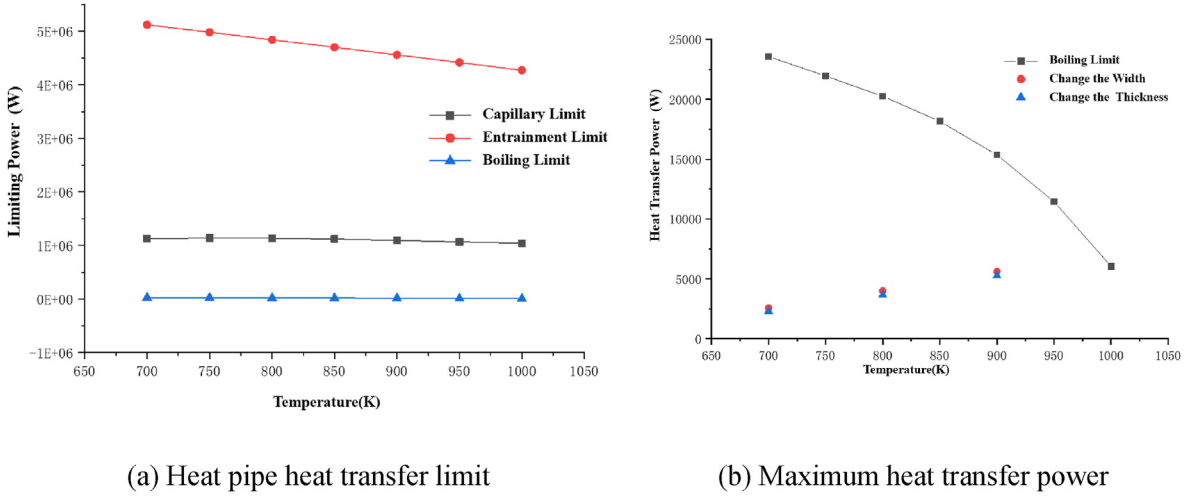

Fig. 9. Heat transfer limit and maximum power.

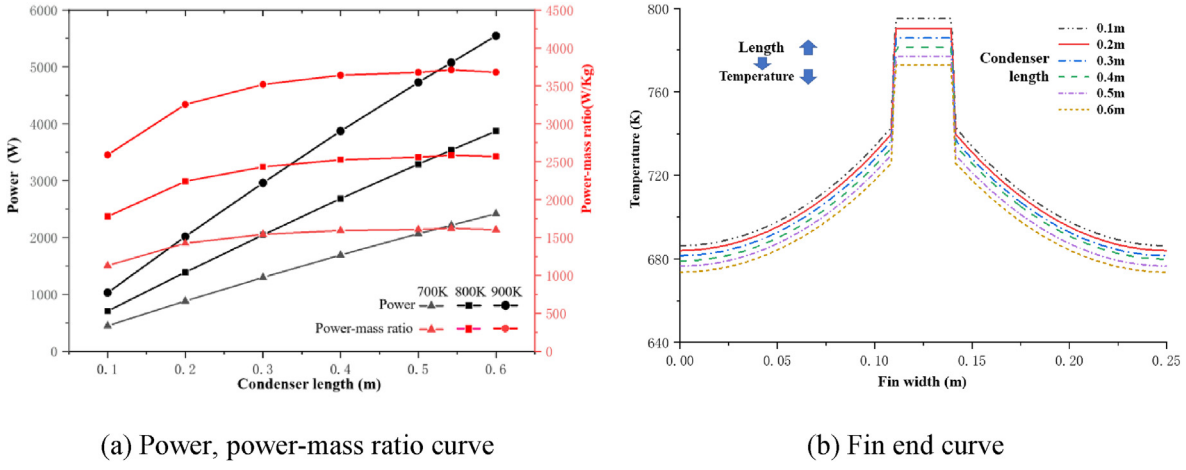

Fig. 10. Comparison of different condensation lengths.

considering the heat transfer limit of the heat pipe, the influence of the heat pipe radius at different temperatures on the heat dissipation power and power-mass ratio are compared as shown in Fig. 11. The radius of the heat pipe mainly affects the temperature of the steam chamber inside the heat pipe. The heat pipe with a larger radius has more working fluids, which can better transmit heat, and

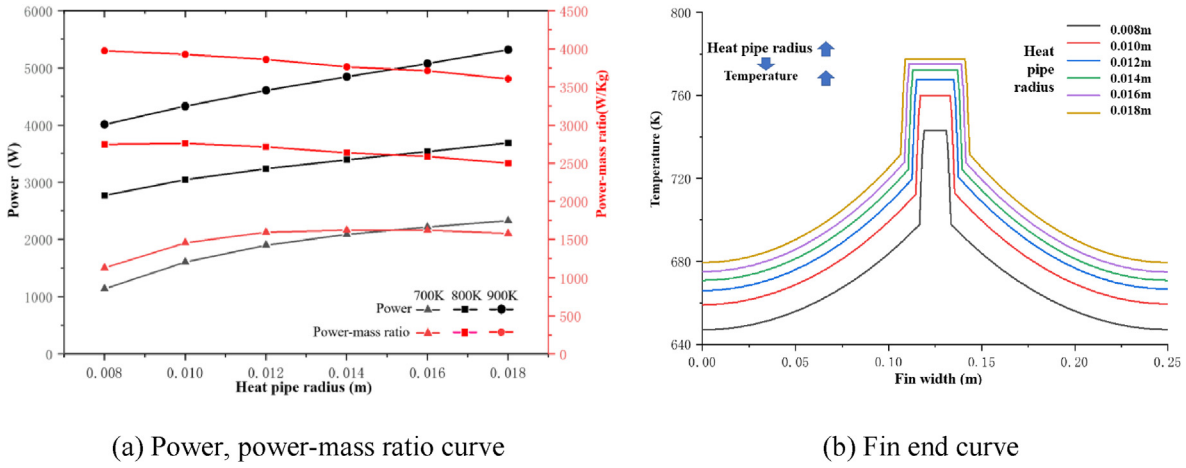

(a) Power, power-mass ratio curve (b) Fin end curve

Fig. 11. Comparison of different heat pipe radius.

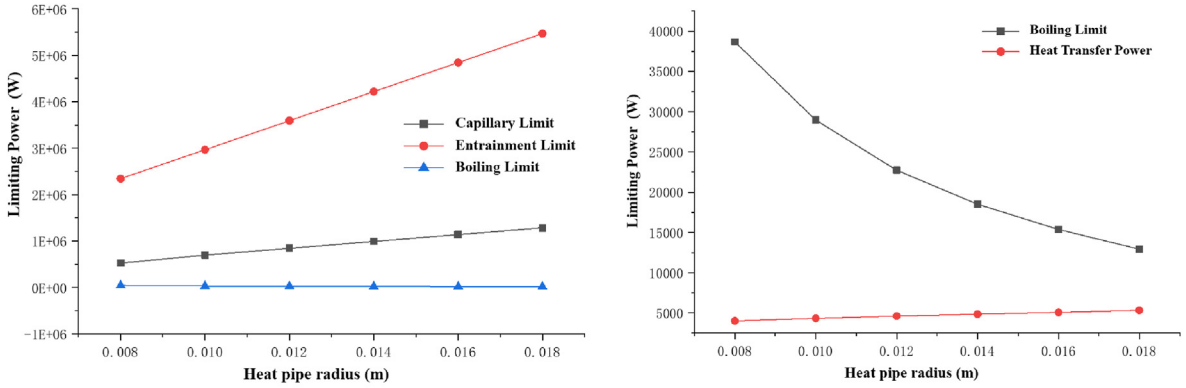

(a) The limit varies with radius (b) Maximum heat transfer power

Fig. 12. Comparison of different heat pipe radius.

the temperature of the steam chamber is higher. However, as the radius increases, the steam temperature increases slowly. The rate of growth of radiative dissipation power will slow down. When temperature of evaporation is 700 K, the power-mass ratio firstly increases and then decreases, and the power-mass ratio is the highest when the radius is 0.014 m. When temperature of evaporation is 800 K, the average power increases by 42.65%, and when temperature of evaporation is 900 K, the average power increases by 43.29% compared with that at 800 K. In the range of analysis, the heat dissipation power of fins increases steadily. However, with the increase of radius, the mass of the combination increases continuously, the power-mass ratio decreases continuously.

It is found that the capillary limit and entrainment limit is increase with the increase of heat pipe radius, while the boiling limit is decreases with the increase of heat pipe radius. The boiling limit is still the minimum heat transfer limit as shown in Fig. 12. The boiling limit decreases with the increase of temperature, while the heat transfer power of the heat pipe increases with the increase of temperature. Therefore, comparing the heat transfer power at 900K temperature can confirm whether the heat pipe reaches its limit. Comparing the maximum heat transfer power of the 900K heat pipe, the boiling limit is greater than the maximum heat transfer power of the heat pipe. So the heat pipe won't break down.

4. Conclusion

Based on MOOSE platform, the simulation heat transfer program of space radiation radiator combination of heat pipe and fin is developed. The calculation time of the newly developed program is compared with that of the traditional multi-physics numerical calculation program, and the accuracy of the numerical calculation is verified. The effects of fin width, fin thickness, condensation section length, and heat pipe radius on the combination's mass and radiation power are analyzed according to the program calculation results. The concept of power-mass ratio is introduced to analyze the influence of different parameters on the heat dissipation power per unit mass. Several conclusions are summarized as follows.

1) The calculation speed of the developed program based on the modular concept increases significantly without reducing the accuracy of the calculation results.
2) Under fixed constraints, when the fin width is 0.25 m, the fin thickness is 0.002 m, the condensing section length is 0.5425 m, and the heat pipe radius is 0.014 m, the work-mass ratio is the highest.
3) In the above temperature range, when the operating temperature increases by 100 K, the heat dissipation power increases by

41.12%. The higher temperature is beneficial to improve the power-mass ratio.

4) When the radiator is designed at a certain temperature, the smaller fin width is used, the thinner fin thickness can improve the power-mass ratio and reduce the radiator quality.

CRediT authorship contribution statement

Xiaoquan Chen: Data curation, Formal analysis, Writing – original draft. **Peng Du:** Writing – review & editing. **Rui Tian:** Investigation. **Zhuoyao Li:** Methodology. **Hongkun Lian:** Validation. **Kun Zhuang:** Data curation. **Sipeng Wang:** Conceptualization, Resources, Supervision.

Declaration of competing interest

The authors declare that they have no known competing financial interests or personal relationships that could have appeared to influence the work reported in this paper.

Acknowledgments

This work is supported by the Fundamental Research Funds for the Central Universities (Grant No. NJ2022019-4).

References

[1] Yong Li, Cheng Zhou, Lv Zheng, etc. Research progress of propulsion technology for high power space nuclear power, [J].Propulsion technology 41 (1) (2020) 12–27.
[2] W. Zhang, C. Wang, R. Chen, et al., Preliminary design and thermal analysis of a liquid metal heat pipe radiator for TOPAZ-II power system[J], Ann. Nucl. Energy 97 (2016) 208–220.
[3] Zhiwen Dai, Tiancai Liu, Chenglong Wang, etc.Study on thermal-hydraulic characteristics of space nuclear reactor power supply, [J].Atom energy science and technology 53 (7) (2019) 1296–1309.
[4] M. Houts, Space Nuclear Power and Propulsion: Materials Challenges for the 21st Century[J], 2008.
[5] M.S. EL-Genk, J.M.P. Tournier, SAIRS" - scalable amtec integrated reactor space power system[J], Prog. Nucl. Energy 45 (1) (2004) 25–69.
[6] L. Mason, C. Carmichael, A Small Fission Power System with Stirling Power Conversion for NASA Science Missions: Nuclear and Emerging Technologies for Space Meeting, NETS-2011[C], 2011.
[7] J.M. Tournier, M.S. EL-Genk, Reactor Lithium Heat Pipes for HP-STMCs Space Reactor Power System[J], Aip Conference Proceedings, 2004.
[8] D.I. Poston, The Heatpipe-Operated Mars Exploration Reactor (HOMER)[J], AIP Conference Proceedings, 2001.
[9] Richter R. 7 0 -s V 6 V a I M 90-1772 Thermody(namic aspects of heat pipe operation[J]).
[10] Y.A.L.E.G. Eastman, The heat pipe[J], Sci. Am. 218 (5) (1968) 38–47.
[11] C.H. Yang, Thermal Analysis of Heat-Pipe Radiators with a Rectangular Groove Wick Structure, Master's thesis[J], 1990.
[12] Xiu Zhang, Haochun Zhang, Xiuting Liu, et al., Thermal analysis and parameter optimization of a heat pipe radiator for space nuclear power [J], Journal of Astronautics (4) (2019) 7.
[13] Hao-chun Zhang, Xiu-ting Liu, Wei Qian-ming, et al., Analysis and optimization of heat pipe radiation radiator for MW space nuclear reactor system [J], Atomic Energy Sci. Technol. 54 (7) (2020) 7.
[14] Z. Tian, Y. Liu, C. Wang, et al., Single/multi-objective optimization and comparative analysis of liquid-metal heat pipe, Int. J. Energy Res. (2022) 1–19, https://doi.org/10.1002/er.8420.
[15] K.K. Panda, I.V. Dulera, A. Basak, Numerical simulation of high temperature sodium heat pipe for passive heat removal in nuclear reactors[J], Nucl. Eng. Des. 323 (nov) (2017) 376–385.
[16] Zhixing Tian, Liu Xiao, Chenglong Wang, et al., Study on heat transfer performance of high temperature potassium heat pipe at steady state [J], Atomic Energy Sci. Technol. 54 (10) (2020) 8.
[17] Yan Shen, Hong Zhang, Hui Xu, et al., Simulation and experimental analysis of heat transfer characteristics of alkali metal heat pipes [J], Journal of solar energy 37 (3) (2016) 7.
[18] q c Chen, Research on heat pipe technology and performance analysis code[J], Atomic Energy Sci. Technol. 54 (7) (2020) 1176–1184.
[19] Baohua Chai, Kaiwen Du, Wei Guangren, et al., Steady numerical analysis of potas sium heat pipe, [J]. Atomic energy science and technology 44 (5) (2010) 5.